

Phase-field Simulation of Recrystallization Based on the Unified Subgrain Growth Theory

Yoshihiro SUWA*

Abstract

Recrystallization occurring in the steel manufacturing process is one of the most important phenomena in order to control the polycrystalline microstructure. This manuscript highlights a unified theory for continuous and discontinuous annealing phenomena by means of the subgrain growth mechanism. In Chapter 2, the mean field analysis based on the unified theory is reviewed. In the analysis, the possibility of abnormal subgrain and/or grain growth based on non-uniform grain boundary mobility and energy has been clearly shown. Subsequently, the numerical simulation results based on the unified theory are outlined. Finally, in Chapter 3, the numerical simulation results of static recrystallization by coupling the unified sub-grain growth theory with the phase-field methodology are discussed.

1. Introduction

When a metal material is subjected to plastic deformation, the internal energy of the material increases due to many lattice defects that are introduced into the crystals, and the material is hardened. When the crystals are heated, the lattice defect density decreases and the material is softened. Such energy release process includes recovery, recrystallization, and grain growth, and plays a vital important role in the microstructural control of polycrystalline materials.¹⁾ The cost will be high if the optimum annealing conditions that differ depending on the steel grade are experimentally derived, and there are limitations to the optimization of conditions using empirical relationships. Accordingly, the development of models for the prediction of recovery, recrystallization, and grain growth based on physical metallurgy is urgently required.

The behavior of recrystallization can be divided into discontinuous recrystallization and continuous recrystallization in appearance. The discontinuous recrystallization is caused by the growth of new grains that are generated in deformed microstructure and have low dislocation density. Usually, recrystallization refers to this discontinuous recrystallization. On the other hand, the continuous recrystallization is a phenomenon in which the dislocation cells or subgrains (SGs) formed by deformation grow as-is into grains. In this paper, the continuous recrystallization means SG growth in the same mechanism as that of normal grain growth not through nucleus for-

mation and growth, and it is not taken into consideration that a low angle boundary (SG boundary) changes to a high angle boundary (grain boundary) during recrystallization. In addition, the distinction between the continuation and discontinuity is purely phenomenological, and the existence of microscopic mechanisms to distinguish these two has not been clarified.²⁾ Furthermore, when considering modeling of the recrystallization behavior, the representation method of nucleation in discontinuous recrystallization currently remains the most important issue.³⁾

About 20 years ago, Humphreys devised a unified theory for continuous and discontinuous annealing phenomena by means of the SG growth mechanism that had been analyzed as individual phenomena until then.²⁾ In their mean field analysis, the possibility of the abnormal growth of a specific SG (i.e., the nucleation of discontinuous recrystallization) can be expressed using the SG interfacial energy and mobility that differ according to the inter-subgrain misorientation. As this SG growth model by Humphreys can represent the spontaneous nucleation behavior of recrystallization including the orientation of recrystallization nuclei, many researchers have tried to simulate the recrystallization behavior using the Monte Carlo (MC) model⁴⁻⁷⁾ and the Vertex model⁸⁻¹⁰⁾ as microstructure calculation techniques based on this model to date.

The content of this paper is organized as follows. In Chapter 2, the SG growth model²⁾ by Humphreys, which has played an impor-

* Senior Researcher, Dr.Eng., Fundamental Metallurgy Research Lab., Advanced Technology Research Laboratories
1-8 Fuso-cho, Amagasaki, Hyogo Pref. 660-0891

tant role in the consideration of the recent recrystallization models is outlined, illustrating the previous studies that combined the SG growth model with microstructure calculation techniques. In Chapter 3, we discuss the main calculation results^{11, 12)} of our recrystallization behavior prediction conducted by coupling the SG growth model with the phase-field (PF) methodology. In Chapter 4, this paper is concluded. This paper is partly excerpted from our report¹³⁾ in Tetsu-to-Hagané, and reconstituted for Nippon Steel & Sumitomo Metal Technical Report.

2. Unified SG Growth Model

As described in the Introduction, Humphreys, about 20 years ago, proposed an idea that allowed for integrated modeling of the process that starts from the nucleation in recrystallization to the grain growth after the primary recrystallization, regardless of continuous or discontinuous recrystallization.²⁾ In this chapter, an outline of this SG growth model is given. Incidentally, Rollett and Mullins devised a model that was on par with Humphreys' model around the same time separately from the study by Humphreys.¹⁴⁾

With deformed microstructure in which the rearrangement of dislocations has progressed to a certain extent, the microstructure is referred to as an aggregation of SGs.¹⁾ When such aggregation of SGs is annealed, the substantially uniform coarsening of all SGs constitutes a continuous phenomenon as (a), (b) in Fig. 1; and the abnormal coarsening of a specific SG alone constitutes a discontinuous phenomenon as (c), (d) in Fig. 1. In the case of the continuous phenomenon, both the SG growth (continuous recrystallization) and normal grain growth can be expressed using the interface misorientation and the scale of the targeted space. Similarly, in the case of the discontinuous phenomenon, the discontinuous recrystallization (primary recrystallization) and the abnormal grain growth (secondary recrystallization) can be expressed.

Now, we will consider the model using Fig. 2 as a system comprising the minimum required components for analysis. The cells in Fig. 2 represent SGs or grains. Actual cells that make up a system have various sizes and interface properties. However, for simplicity, the component elements of the system here are limited to the aggregation of the cells that has an average grain size $\langle R \rangle$ and an average misorientation $\langle \theta \rangle$ (thus, interface energy $\langle \gamma \rangle$, interface mobility $\langle M \rangle$), as well as a single cell that has the properties (R, θ, γ, M) different from those of the aggregation of the cells.

The assumption of a cellular microstructure as described above is considered to be appropriate for the alloys of high stacking fault energy with the relatively small additive elements (e.g., most aluminum alloys and ferritic steel) deformed at relatively high temperature. However, the modeling cannot be a good approximation for metals of low stacking fault energy deformed at low temperatures. Recently, Zurob, et al. have devised a model that is applicable to even alloys with low stacking fault energy by considering the time variation of the dislocation density existing in cells.¹⁵⁾

Due to space limitations, here we describe the results without detailing the process. The ratio between the growth rates of a cell aggregation and a grain abnormally growing is calculated by the following equation.

$$\frac{d}{dt} \left(\frac{R}{\langle R \rangle} \right) = \frac{1}{R^2} \left(\langle R \rangle \frac{dR}{dt} - R \frac{d\langle R \rangle}{dt} \right) \quad (1)$$

From this equation, the condition under which the microstructure loses the stability and the discontinuous growth occurs can be expressed by the following equation.

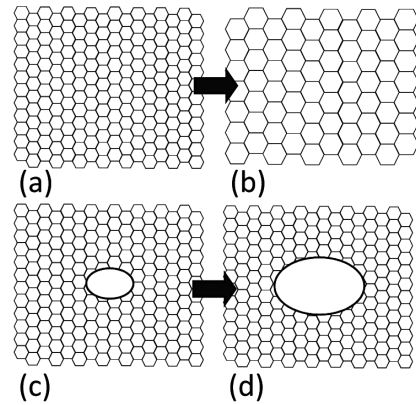


Fig. 1 Schematic illustration of (a, b) continuous and (c, d) discontinuous annealing phenomena

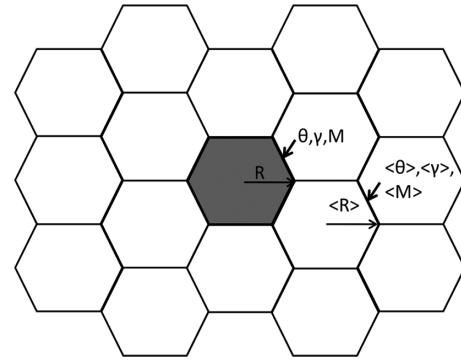


Fig. 2 Idealized cellular microstructure assumed in the mean field analysis
Grains are approximated to spheres of radii R and $\langle R \rangle$.

$$\langle R \rangle \frac{dR}{dt} - R \frac{d\langle R \rangle}{dt} > 0 \quad (2)$$

When substituting the expressions¹⁶⁾ for dR/dt and $d\langle R \rangle/dt$ derived by Hillert into the above equation, the following equation is obtained.

$$M\langle \gamma \rangle - \frac{\langle R \rangle M \gamma}{R} - \frac{R\langle M \rangle \langle \gamma \rangle}{4\langle R \rangle} > 0 \quad (3)$$

In order to simplify the representation, equation (3) is rewritten using the relative values as follows.

$$X = \frac{R}{\langle R \rangle}, \quad Q = \frac{M}{\langle M \rangle}, \quad G = \frac{\gamma}{\langle \gamma \rangle} \quad (4)$$

When using these values, equation (3) becomes

$$Y = 4QX - 4QG - X^2 > 0 \quad (5)$$

If $Y=0$, the following equation is satisfied.

$$X = 2Q \pm 2(Q^2 - QG)^{1/2} \quad (6)$$

The two solutions of equation (6) give the boundary values as to whether the grain growth becomes discontinuous.

The conditions that make the growth discontinuous depend on the relative values X , G , and Q of grain size, interface energy and mobility, respectively. Figure 3 shows the relationships of Q values and the attainable size ratios X for the various values of G . Looking at Fig. 3, when M and G are fixed, the attainable size ratio due to the

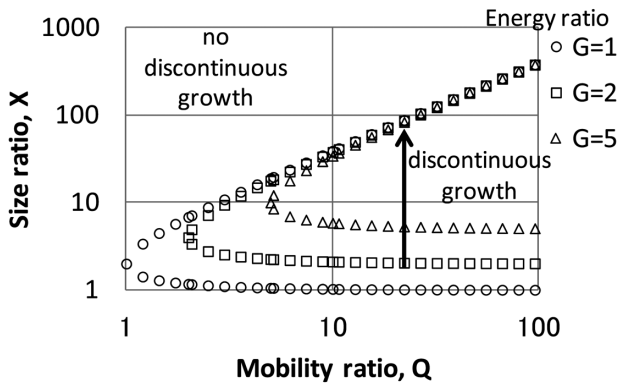


Fig. 3 Conditions for discontinuous growth as a function of the relative sizes (X), boundary energies (G) and mobilities (Q) of the grains. Stating point and end point of the arrow in the figure indicate the minimum value required for abnormal growth and the maximum value attained in abnormal growth, respectively.

discontinuous growth is indicated as well as the size ratio required for discontinuous growth. After the size ratio reaches the attainable maximum value, the growth proceeds while X is maintained at a constant value. Generally, the discontinuous growth is likely to occur when the X and M values are large while the G values are small. However, if the interface energy and the interface mobility of SG boundaries are the functions of misorientation θ , it is difficult for a situation in which M values are large and G values are small to be realized. Humphreys mainly discussed the stability of SG structure and the possibility of recrystallization due to the strain-induced grain boundary migration (SIBM) using equation (6) and the boundary mobility and energy as a function of the misorientation.²⁾ Furthermore, the analysis in consideration of the grain boundary pinning due to the precipitated second phase¹⁷⁾ was also performed.

The above model is an excellent one, but uses simplified microstructure, which makes it difficult to analyze explicitly considering the local arrangement of individual SGs. Many researchers have conducted the numerical calculations of recrystallization behavior considering the SG structure since Humphreys presented the SG growth model. As the research focusing on the nucleation process of discontinuous recrystallization, Holm, et al.⁴⁾ used the MC model for discussing the nucleation of discontinuous recrystallization in single crystals using the crystal orientation distribution obtained from the experiment.

With the Vertex model, Weygand, et al.⁹⁾ investigated the effect of SG structure on the SIBM of existing grain boundaries, using the bicrystal system composed of the SG structures. Specifically, they conducted calculations while changing the mean SG size in a grain across the existing grain boundary. Humphreys⁸⁾ performed the numerical analysis of the nucleation behavior of recrystallization from the transition band using the Vertex model, considering a single crystal structure taking the transition band into account as the initial structure. As an example of research focusing on the growth process in discontinuous recrystallization (especially the growth at the recrystallization front), Radhakrishnan, et al.⁶⁾ used the MC model in the analysis of the effect of SG structure on the migration velocity of an existing grain boundary (i.e., recrystallization front), while changing the SG structure across existing grain boundaries of a bicrystal, thereby varying the strain energy introduced by deformation.

As a research for polycrystalline microstructure, Weygand, et

al.¹⁰⁾ used the Vertex model in the verification of the conditions under which discontinuous recrystallization is initiated by the nucleation from an existing grain boundary by using the simple initial configurations based on experimental observations. Further, they also derived the Avrami exponent from numerical calculation results. On the other hand, Radhakrishnan, et al.⁷⁾ modeled the deformed microstructure using the crystal plasticity finite-element method (CPFEM), the obtained strain energy distribution and orientation distribution were converted into SG structure, and the recrystallization texture was calculated by the MC model. Furthermore, Takaki, et al.¹⁸⁾ also modeled deformed microstructure using the CPFEM, and converted it into SG structure while maintaining the distributions of strain energy and crystal orientation in order to link the deformed microstructure with the recrystallization model using the PF methodology.

3. PF Simulation of Recrystallization Based on the SG Growth Model

3.1 Model outline and calculation conditions

In this chapter, the results of the recrystallization simulation are discussed. In the simulation, the PF method was combined with the SG growth model and utilized as a microstructure calculation technique. In particular, (i) the recrystallization front velocity when the discontinuous recrystallization occurs¹¹⁾ and (ii) the relationship between the discontinuous/continuous transition of the recrystallization and the fraction of the high-angle grain boundary in the initial structure¹²⁾ are shown. Due to space limitations, we would like to ask readers to refer to individual references¹¹⁻¹³⁾ for more information.

The PF model used to reproduce microstructure evolutions is the modified version of Fan and Chen's model^{19, 20)}. Fan and Chen's model uses many order parameters to express polycrystalline microstructure and the model was extended in order to take the anisotropy in interface mobility and energy into consideration^{21, 22)}. In the model, the excess energy caused by the curvature of interfaces is considered as the driving force of recrystallization. At a low-angle grain and SG boundary ($\theta < \theta_m$), the dependence of the interface mobility and energy on the misorientation was respectively assumed as follows.

For mobility²⁾:

$$L(\theta) = L_0 \left(1 - \exp \left(-5 \left(\frac{\theta}{\theta_m} \right)^4 \right) \right) \quad \theta \leq \theta_m \quad (7)$$

For energy²³⁾:

$$\gamma(\theta) = \gamma_0 \frac{\theta}{\theta_m} \left(1 - \ln \frac{\theta}{\theta_m} \right) \quad \theta \leq \theta_m \quad (8)$$

At a high-angle grain boundary, the dependence of the interface mobility and energy as above was assumed to be constant values L_0 and γ_0 , respectively.

In the numerical calculations, finite difference grid interval Δx and time interval Δt are $\Delta x = 1.0$ and $\Delta t = 0.1$, respectively. Also, in the following discussion, the length and area are indicated in units of the number of grid points (g. p.), and the reference unit of time is (s'). All calculations were performed in two dimensions. The calculation results described in this chapter can be roughly divided into (i) calculations on the time evolution of recrystallization fronts, and (ii) integrated calculations from the nucleation in recrystallization to the grain growth after the recrystallization completion.

For (i), the two-dimensional regions of A, B, and C shown in

Fig. 4 were considered. The region size is 1024^2 . An initial structure was constructed as follows: first, a polycrystalline microstructure was created by simulating normal grain growth with the assigning of one of the groups of orientation. After that, each different orientation was assigned to the regions A and B. The purpose of the simulation was to examine the time evolution at the recrystallization front, i.e., BC interface. Here, A was assumed to be an immovable region, and the interfacial misorientations between A and B and between A and C were $\theta_{AB}=1$ and $\theta_{AC}=1$ (deg), respectively. In addition, $\theta_{BC}>15$, which means that the BC interface is always a high-angle grain boundary, was assumed. Based on these assumptions, the simulation was performed, changing the misorientation θ_{CC} in the SG structure C.

Figure 5 shows the initial structure in the case of (ii) in which a large number of existing grains are present. In this figure, the number of existing grains $N=12$, and the initial mean SG size $\langle R_0 \rangle = 7.42$. The size of the calculation region is 2100^2 , the large polygons are the existing grains in which the small grains that are individual SGs can be seen. The initial configurations were prepared as follows. First, a polycrystalline microstructure was created by simulating normal grain growth under the assumption of a single orientation group for the entire system. Next, all the SGs were divided into 12 groups by using a weighted Voronoi tessellation. The total num-

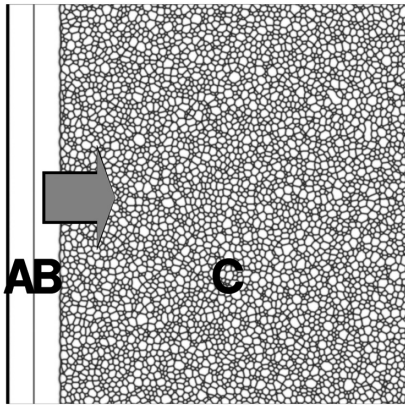


Fig. 4 Schematic illustration of the simulation system with regions A, B and C

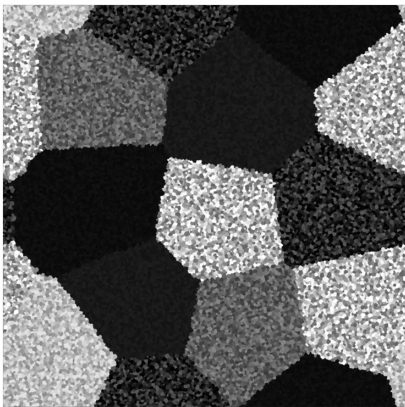


Fig. 5 Initial configuration of the simulation system comprising 12 grains
Calculations were performed on a two-dimensional lattice with a size of 2100^2 (g.p.).

ber of SGs is approximately 23000. Here, only the mechanism in which existing grain boundaries bulge was considered as the nucleation mechanism of recrystallization. The nucleation in discontinuous recrystallization requires the presence of high-angle grain boundaries. In particular, in small strain regions, it has been confirmed experimentally that the existing grain boundaries are important nucleation sites.¹⁾ The differences between a (existing) grain boundary and a SG interface, which were important to the simulation, are defined as follows.^{10, 12)}

- (1) Generally, a grain boundary is a high-angle boundary with high energy and high mobility compared with an SG interface.
- (2) The misorientation at an SG interface is small, and the interfacial energy and interface mobility vary greatly depending on the misorientation.
- (3) Actual misorientation between SGs are dispersed with a certain degree of distribution. However, only one type of SG interface with misorientation θ_{CC} is considered to simplify the calculation. Accordingly, no recrystallization nucleus is formed in existing grains.

Based on these assumptions, the simulation was conducted with the change made in the inter-subgrain misorientation θ_{CC} and the number of existing grains N . The change of these two values along with the progress of deformation has been experimentally confirmed to exert large influence on the recrystallization behavior.^{24, 25)} In particular, this paper discusses the analysis results of the relationship between N and the discontinuous/continuous recrystallization transition.

3.2 Migration velocity of recrystallization fronts in absence of bulk recovery

Prior to the simulation results conducted using the PF method, we evaluate the migration velocity of the recrystallization front using the SG growth model²⁾ by Humphreys. In order to simplify the problem, the microstructure is considered to comprise of only two components: an assembly of cells of mean radius ($\langle R_C \rangle$), boundary type (misorientation $\langle \theta_{CC} \rangle$, energy $\langle \gamma_{CC} \rangle$ and mobility $\langle M_{CC} \rangle$) and SGs that are potential recrystallization nuclei with grain size (R_B) and interface properties (θ_{BC} , γ_{BC} , M_{BC}). Here, assuming $\langle R_C \rangle < R_B$ and $\langle M_{CC} \rangle \ll M_{BC}$, the growth rate of the recrystallization front (i.e., interface between B and C) can be expressed as follows.

$$\frac{dR_B}{dt} = v = \frac{M_{BC} \langle \gamma \rangle}{\langle R_C \rangle} \quad (9)$$

Accordingly, when the grain growth (recovery) in the SG aggregation is negligibly small, the velocity v of the recrystallization front has a constant value in inverse proportion to $\langle R_C \rangle$.

Next, we evaluate our numerical simulation results by using equation (9). Considering the system as shown in Fig. 4, the ratio of the interface mobility ($M_R = \langle M_{CC} \rangle / M_{BC}$) was assumed to be 0.01 in order to suppress the recovery in the SG aggregation C. In addition, the ratio of the interfacial energy ($\gamma_R = \langle \gamma_{CC} \rangle / \gamma_{BC}$) was assumed as 1. Under these conditions, the initial mean SG size $\langle R_C \rangle(0)$ of the aggregation C was changed from 8.12 to 31.6 to perform the calculation. Figure 6 shows the relationship between migration velocity v of the BC interface and $2.0 \langle R_C \rangle(0)$. The average value of $400 < t < 3600$ was used as velocity v . As shown in this figure, except for $\langle R_C \rangle(0) < 12.0$, a linear relationship was obtained, and the migration velocity of the BC interface was a constant value in conformity to equation (9). In the case of $\langle R_C \rangle(0) < 12.0$, it is considered that the linear relationship was not obtained due to the low resolution of the computational grid that was not high enough to describe the curva-

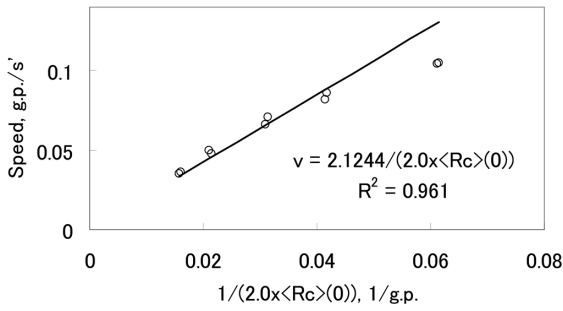


Fig. 6 Relationship between the temporal average of the velocity, $\langle v \rangle$ and the inverse of $2.0 \times \langle R_c \rangle(0)$
Value of $\langle v \rangle$ is obtained by averaging over $400 < t < 3600$ in each simulation run. Solid curve is the results of a least-squares fit of data points in the range $\langle R_c \rangle(0) > 8.0$.

ture of SGs in the aggregation C.

When the recovery in the SG aggregation is obvious, a decline in v involved in the decrease of the driving force can be confirmed using the same model.¹¹⁾ Furthermore, a recent analysis has shown a zigzag pattern of a recrystallization front, for which the cause is still unclear.²⁶⁾

3.3 Influence of total number N of existing grains in polycrystalline microstructure

The total number N of existing grains was adjusted by changing the aspect ratio of existing grains while compressing in the Y-axis direction and maintaining a constant length in the X-axis direction. **Figure 7** shows each initial structure with $N=48$ and $N=192$. **Figure 8** shows the time variation of the mean SG sizes with $N=12$, $N=48$, and $N=192$, using $\theta_{cc}=4$ (deg) and $\langle R_0 \rangle = 7.42$. The percentages of high-angle grain boundaries in the initial structure of these three configurations were 3.2%, 7.7%, 29.8%, respectively. For making a comparison, we have also utilized the initial structure with $N=192$ and the isotropic (i.e. aspect ratio = 1:1) existing grains. This condition will be hereafter referred to as $N=192$ (ISO). In this case, the percentage of the high-angle grain boundaries in the initial structure was 12.7%. If the percentage of the high-angle grain boundaries is small enough, a discontinuous recrystallization takes place and the slope of the growth curve exhibits a great change twice as shown in Fig. 8. In this case, the growth curve can be divided into three regions; the nucleation in the discontinuous recrystallization (beginning of the abnormal grain growth of specific SGs), growth of recrystallization grains, and grain growth after the recrystallization completion.

On the other hand, in the case of $N=192$ where the percentage of the high-angle grain boundaries is highest, the growth curve shows significant deviation from its characteristic of discontinuous recrystallization. The reason for this is as follows. The nucleation site of recrystallization increases along with the increase of N , and the initial recrystallization velocity increases. However, when N increases in excess, existing grain sizes become smaller, resulting in a situation in which the collisions between recrystallized grains are likely to occur. Such collisions prevent the long distance migration of high-angle grain boundaries (i.e., recrystallization fronts). When considered in combination with the results of $N=192$ (ISO), it is contemplated that the percentage of the high angle-grain boundaries rather than the aspect ratio of existing grains dominates the discontinuity of recrystallization.

According to the experimental results of Jazaeri,²⁴⁾ et al., the discontinuous and continuous transition value of recrystallization is a

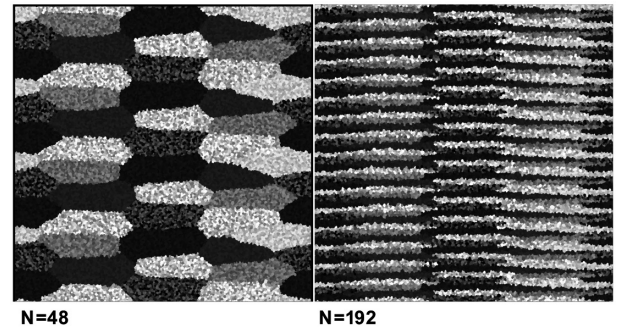


Fig. 7 Initial configurations with $N=48$ and $N=192$
Initial mean subgrain radius, $\langle R_0 \rangle$ is kept constant as $\langle R_0 \rangle = 7.42$. Fraction of high-angle (pre-existing) grain boundaries in the initial structure were 3.2% ($N=12$), 7.7% ($N=48$), 29.8% ($N=192$), and 12.7% ($N=192$ (ISO)).

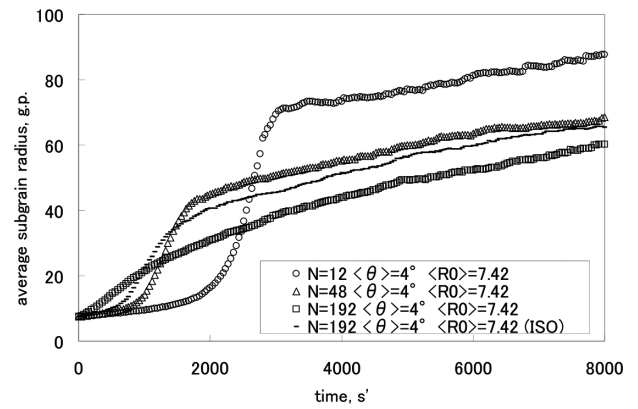


Fig. 8 Temporal evolutions of the mean subgrain radius $\langle R \rangle$ for various values of N
In the case of $N=192$, the obtained recrystallization curve exhibits significant deviations from a sigmoidal shape.

high-angle boundary percentage at 60%. However, this threshold greatly depends on the definition of the discontinuous recrystallization as well as the target material. At least, the calculation results in this section showed the suppression of discontinuous recrystallization because of the enlargement of the high-angle boundaries.

4. Conclusion

In this paper, we illustrated the models that can predict the unified process from the nucleation of the recrystallized grain to the grain growth after the recrystallization by considering SG structures. In particular, we outlined the SG growth model of Humphreys²⁾, which played an important role in considering the recent recrystallization models, and described our simulation results^{11, 12)} of recrystallization behavior conducted by using the phase-field (PF) method for microstructure calculation based on the SG growth model. As the characteristics of this model make consideration of individual SGs necessary, the calculation cost becomes enormous. Consequently, even if the parallelization of numerical calculations and the improvement of algorithms are performed, the calculations will unavoidably take long periods of time. Considering the practical utility, we believe that appropriate uses of the SG growth model should be considered, for example, the use for the parameter derivation in a Kolmogorov-Johnson-Mehl-Avrami (KJMA) model²⁷⁾.

In addition, such an approach can allow us to separate phenome-

na that can be fully represented by a KJMA model from those that cannot be reproduced without considering the SG structure explicitly. While this report does not describe the time evolution of the texture during recrystallization, it has been made possible to perform the three-dimensional analysis of recrystallization behavior (including the texture change) using the PF method in which the actual crystal orientation is considered.²⁶⁾

When performing the recrystallization analysis starting from SG structures, the most important thing is the means for obtaining deformed microstructure as the initial values of the calculations. One of the methods²⁸⁾ is to use the crystal orientation distribution measured though the electron backscatter pattern (EBSP) method. On the other hand, as a usage of numerical calculations, there is a method to reproduce deformed microstructure through the CPFEM as described in Chapter 2. For the integrated analysis from deformation to annealing, it is necessary to develop a model for the prediction of microstructural evolution during deformation that can capture the formation of a heterogeneous deformation region around a grain boundary and coarse precipitate or shear band, in conjunction with the approach described above. This is because the heterogeneous deformation region and the shear band are preferential nucleation sites of discontinuous recrystallization. Finally, the recrystallization behavior prediction model based on the SG growth model introduced in this paper is premised on the existence of SGs in the initial configuration. As already described, this premise is not always possible. Accordingly, the development of a simulation method that includes the SG formation process is also a future challenge.

References

- 1) Humphreys, F.J., Hatherly, M.: Recrystallization and Related Annealing Phenomena. Oxford, Pergamon, 1995
- 2) Humphreys, F.J.: Acta Mater. 45, 4231 (1997)
- 3) Humphreys, F.J.: Mat. Sci. Forum. 467-470, 107 (2004)
- 4) Holm, E.A. et al.: Acta Mater. 51, 2701 (2003)
- 5) Okuda, K., Rollett, A.D.: Mat. Sci. Forum. 408, 413 (2002)
- 6) Radhakrishnan, B., Zacharia, T.: Model Simul. Mater. Sci. Eng. 11, 307 (2003)
- 7) Radhakrishnan, B. et al.: Scripta Mater. 39, 1639 (1998)
- 8) Humphreys, F.J.: Scripta Metall. 27, 1557 (1992)
- 9) Weygand, D. et al.: Phil. Mag. B80, 1987 (2000)
- 10) Weygand, D. et al.: Interface Sci. 9, 311 (2001)
- 11) Suwa, Y. et al.: Mat. Sci. Eng. A457, 132 (2007)
- 12) Suwa, Y. et al.: Com. Mat. Sci. 44, 286 (2008)
- 13) Suwa, Y.: Tetsu-to-Hagané. 97, 173 (2011) (in Japanese)
- 14) Rollett, A.D. et al.: Scripta Mater. 36, 975 (1997)
- 15) Zurob, H.S. et al.: Acta Mater. 54, 3983 (2006)
- 16) Hillert, M.: Acta Metall. 13, 227 (1965)
- 17) Humphreys, F.J.: Acta Mater. 45, 5031 (1997)
- 18) Takaki, T., Tomita, Y.: Int. J. Mech. Sci. 52, 320 (2010)
- 19) Fan, D., Chen, L.Q.: Acta Mater. 45, 611 (1997)
- 20) Fan, D. et al.: Mater. Sci. Eng. A238, 78 (1997)
- 21) Kazaryan, A. et al.: Acta Mater. 50, 2491 (2002)
- 22) Ma, N. et al.: Acta Mater. 52, 3869 (2004)
- 23) Read, W.T., Shockley, W.: Phys. Rev. 78, 275 (1950)
- 24) Jazaeri, H., Humphreys, F.J.: Acta Mater. 52, 3239 (2004)
- 25) Jazaeri, H., Humphreys, F.J.: Acta Mater. 52, 3251 (2004)
- 26) Suwa, Y. et al.: CAMP-ISIJ. 28, 891 (2015), CD-ROM
- 27) Zurob, H.S., Hutchinson, C.R., Brechet, Y., Purdy, G.: Acta Mater. 50, 3075 (2002)
- 28) Baudin, T. et al.: Scripta Mater. 32, 63 (2000)



Yoshihiro SUWA
Senior Researcher, Dr. Eng.
Fundamental Metallurgy Research Lab.
Advanced Technology Research Laboratories
1-8 Fuso-cho, Amagasaki, Hyogo Pref. 660-0891